

3D Printed Prototype of an EMG-Controlled Bionic Forelimb for Amputee Cats

Noureddine RABAH-SIDHOUM^{1,2}, Ryhane BOUABDELLAH³,
Mehdi BOUCHEIKHCHOUKH¹, Noureddine MECOUK⁴

¹Department of Veterinary Sciences, Chadli Bendjedid El Tarf University, Algeria.

²Biodiversity and Ecosystems Pollution Laboratory, Faculty of Life and Nature Sciences,
Chadli Bendjedid University, El Tarf, Algeria.

³Clinic Department, National Higher School of Veterinary Medicine Rabie Bouchama,
Algiers Algeria.

⁴Ecology of Terrestrial and Aquatics Systems Laboratory (EcoSTaQ), Department of Biology,
Faculty of Science, Badji Mokhtar University, Annaba 23200, Algeria.

Email: n.rabah-sidhoum@univ-eltarf.dz

Abstract - In this study, an orthopedic and biomechanical characterization of the domestic cat's forelimb was undertaken. Subsequently, a 3D-printed prototype was developed for the cat's forelimb using fused deposition modeling with Polyethylene Terephthalate Glycol-Modified material, leveraging measurements from five adult cats. The resulting prototype comprises a comprehensive bionic system, replacing carpal and metacarpal articulations with servomotors, and is controlled by an Arduino Uno R3 using EMG signals.

Keywords – Algeria, bionic limb, cat, EMG, orthopedic.

I. INTRODUCTION

A prosthesis serves as an artificial substitute for a missing body part, preventing deformation and degeneration of existing joints in limb amputees. Limb prostheses provide various benefits, including addressing leg length discrepancies, enhancing exercise and activity levels, and facilitating participation in rehabilitation therapy and daily living activities (Jarrell & Farrel, 2018).

In humans, limb prostheses are sometimes secured using hermetic seals created by suction and gel sheaths. However, this method is impractical for small animals due to their fur, limiting the feasibility of prosthetic use (Ishmael et al., 2019). Contrastingly, bionic limbs present several advantages (Durfée & Iaizzo, 2019). Firstly, fitting a bionic limb onto an animal is a more straightforward process.

The aesthetic appeal of a bionic limb is undeniable, contributing to the overall well-being of the animal by facilitating its reintegration into its environment. Additionally, the use of bionic limbs reduces the risks associated with graft rejection and overall costs. Notably, bionic prostheses are designed to restore more than 95% of the limb's original activity.

It is crucial to consider not only the functional aspects but also the behavioral response of the animal to the prosthesis. Cats, for example, wearing passive titanium transtibial prostheses, exhibit positive adaptation, utilizing a quadruped gait and relying on the prosthesis for mobility (Jarrell & Farrel, 2018). The design of a prosthesis, therefore, goes beyond merely substituting a limb; it must account for the animal's behavior to enhance its overall quality of life.

The aim of this study is to model and produce a prototype of a bionic prosthesis for the cat's

forearm and then apply it through clinical tests on amputee cats. Our goal is to produce a biomedical prototype that can be upgraded with more sophisticated, industrially adapted equipment. Aspects such as measurements of the cat's muscular activity, design, assembly, and programming were considered.

II. MATERIAL AND METHODS

This study were conducted in the first semester of 2021, five Adult cats including two males and three females of European breed were examined and measures of scapular, humeral, radio-ulnar and paw length were taken. After that, a technical design using Blender v2.76 3D software was prepared for three substituting parts of the forelimb, which are to date the socket, the radio-ulnar substitute, and the paw based on the average measures.

A) Biomechanical characterization of the forelimb movement

Analyzing the cat forelimb from a mechanical standpoint allow basically the understanding of the forces and torques that govern the different parts of the limb to allow an optimal choice and modelling of the parts including the servomotors, the forelimb can be segmented into three distinct segments starting from its distal end. These segments are as follows: the first segment corresponds to the structures of the metacarpus and phalanges, the second segment corresponds to the assembled radius and ulna, and the third segment corresponds to the humerus. Each of these bones is connected to the one preceding it by an articulation with a well-defined angle of rotation along its vertical axis. The angles θ_2 , θ_3 , and θ_4 represent the respective angles at the wrist, elbow, and shoulder joints, while the angle θ_1 is formed by the axis of the carpal structures and the supporting surface of the limb.

We adopted Xueqing Wu's 2019 assumptions for the dynamic study: treating each cat as a rigid body model with planar link segments, considering limb segments as working independently under a combination of joint

forces, muscle moments, and gravity, and focusing solely on vertical joint reaction forces relative to the Earth's surface, as it appears in figure 1.

According to the second fundamental principle of dynamics;

$$\sum F = ma \quad (1)$$

Thus, by projection onto the two axes of the orthonormal reference frame, we obtain the two formulas:

$$\sum F_x = ma_x = F_{x_p} - F_{x_d} \quad (2)$$

$$\sum F_y = ma_y = F_{y_p} - F_{y_d} - mg \quad (3)$$

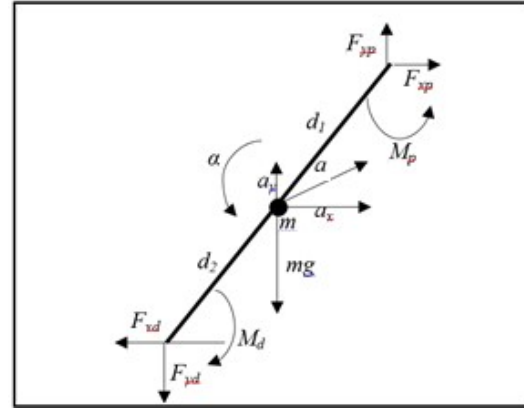


Fig. 1. Free-body diagram of a single limb segment illustrating forces, moments, linear and angular accelerations.

By applying, the angular momentum theorem applied to segment AB:

$$M = M_i \alpha \quad (4)$$

Where M_i and M are respectively the moments of inertia and angular momentum of the segment AB on the plane of motion. By applying formulas 2, 3 and 4 to each segment, we obtain for each segment respectively;

$$F_{1x} = m_1 \left(\frac{-L_1}{2} (\theta_1')^2 \cos \theta_1 - \frac{L_1}{2} (\theta_1'') \sin \theta_1 \right) \quad (5)$$

$$F_{1y} + F_{1y} - m_1 \cdot g = m_1 \left(-\frac{L_1}{2} (\theta_1')^2 \sin \theta_1 + \frac{L_1}{2} (\theta_1'') \cos \theta_1 \right) \quad (6)$$

$$M_1 + F_{1x} \frac{L_1}{2} \sin \theta_1 + F_{1y} \frac{L_1}{2} \cos \theta_1 - F_{1y} \frac{L_1}{2} \cos \theta_1 = -I_1 \theta_1'' \quad (7)$$

$$F_{2x} - F_{1x} = m_2 \left[-L_1 ((\theta_1')^2 \cos \theta_1 + (\theta_1'') \sin \theta_1 - \frac{L_2}{2} ((\theta_2')^2 \cos \theta_2 + \theta_2'' \sin \theta_2) \right] \quad (8)$$

$$F_{2y} - F_{1y} - m_2 g = m_2 [L_1(-(\theta_1')^2 \sin \theta_1 + \theta_1'' \cos \theta_1) + \frac{L_2}{2}(-(\theta_2')^2 \sin \theta_2 + \theta_2'' \cos \theta_2)] \quad (9)$$

$$M_2 - M_1 + \frac{L_2}{2} F_{2x} \sin \theta_2 - F_{2y} + \frac{L_2}{2} \cos \theta_2 + F_{1x} + \frac{L_2}{2} \sin \theta_2 - F_{1y} + \frac{L_2}{2} \cos \theta_2 = -I_2 \theta_2 \quad (10)$$

$$F_{3x} - F_{2x} = m_3 [-L_1((\theta_1')^2 \cos \theta_1 + \theta_1'' \sin \theta_1) - 2L_2 \theta_2 \cos \theta_2 + \theta_2 \sin \theta_2 + 4L_3 \theta_3 \cos \theta_3 + \theta_3 \sin \theta_3] \quad (11)$$

$$F_{3y} - F_{2y} - m_3 g = m_3 [L_1(-(\theta_1')^2 \sin \theta_1 + \theta_1'' \cos \theta_1) + L_2(-(\theta_2')^2 \sin \theta_2 + \theta_2'' \cos \theta_2) + \frac{L_3}{2}(-(\theta_3')^2 \sin \theta_3 + \theta_3'' \cos \theta_3)] \quad (12)$$

$$M_3 - M_2 + F_{3x} \frac{L_3}{2} \sin \theta_3 + F_{3y} \frac{L_3}{2} \cos \theta_3 + F_{2x} \frac{L_3}{2} \sin \theta_3 + F_{2y} \frac{L_3}{2} \cos \theta_3 = I_3 \theta_3 \quad (13)$$

3D models of each part are depicted in Fig. 1.

The printing process was realized using fused deposition modelling (FDM) technology; the choice of the material used for 3D printing was qualitative; in fact, we wanted a resistant but flexible material in order to facilitate any necessary modifications after printing and to avoid the risk of breaking the part B that is quite longer than the rest of parts. Thus, the material of choice was glycosides polyethylene terephthalate (GPET).

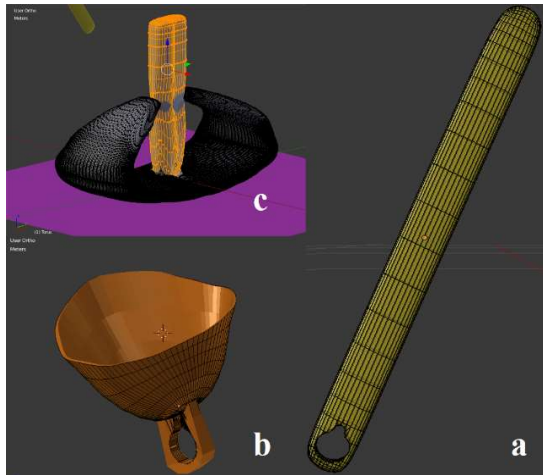


Fig. 2. Perspective view of : a. the forearm substitute b. the elbow fitting c. the limb end substituent.

Figure 3 include all key-steps followed in the conception of the prototype.

After printing, the parts were cleaned painted and assembled with servomotors SG90 on the other hand one male of the five cats was

considered for surface electromyography (sEMG) signal measures using muscle sensor V3 developed by (Advancer technologies ©)

The penultimate step consists of assembling everything in order to carry out clinical and biomechanical tests of the prototype in order to adjust and improve the product (Thakor & Cabibihan, 2018). For some steps such as measuring muscle, activity pre-requisite knowledge is required.

B) Preparing the patient for surface electromyography

The preparation of the patient for surface electromyography follows certain rules in order to record good quality signals (Konrad, 2005):

- The area where the surface electrode is to be positioned must be well shaved or mown.

The skin should be cleansed with alcohol or hydro-alcoholic gel, using circular movements until the skin takes on a rosy hue. This cleansing removes dirt, dead skin debris that increase the impedance of the skin, thus affecting the quality of the signal. It is important to avoid rubbing too hard when cleaning.

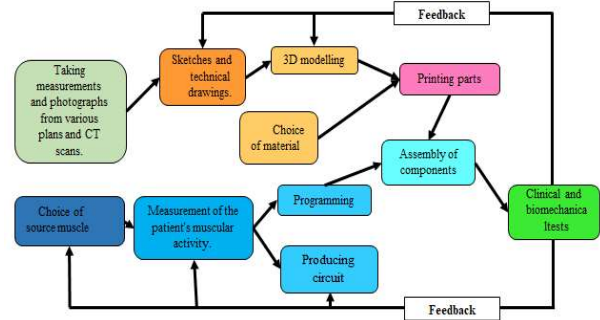


Fig. 3. Flow chart of the stages involved in the design of support parts and their biomedical and electronic production.

- To avoid causing lacerations that will affect the signal obtained from the concerned area.
- The electrodes must be placed close together, preferably aligned so that the red and yellow electrodes are juxtaposed on the same muscle; the green reference electrode is placed on the tendon close to the radio-ulnar joint. Incorrect placement of the electrodes

would give a non- representative signal and increase the chances of obtaining artefacts due to interference from other signals from neighbouring motor units (for example a signal from a triceps UM) or even from a nerve.

- Once the electrodes have been positioned, the code can be uploaded to the microcontroller.
- Data can be visualised as a graph on the serial plotter in the tools section, or as figures characterising the amplitudes by clicking on the serial monitor option.
- When reading the trace, it is important to distinguish between artefacts caused by the circuit, electrode movement and ECG artefact.

C) Measurements

The average length of each part of the forelimb and the circumference of the arm taken as reference for the design, are depicted in table I.

Table I. Representation of the length, circumference, weight and their averages for the 5 cats. L_{g-e} : Length from withers to shoulder, L_{e-c} : length from shoulder to elbow, L_{c-w} : length from elbow to wrist, L_{w-p} : length from wrist to middle phalanx, L_{p-p} : length from middle phalanx to end of third phalanx.

C	Report of the animal	weight	Dimensions	Circumference	Average
1	Male, 4 years old, vaccinated	4.7kg	$L_{g-e}=8.5\text{cm}$ $L_{e-c}=10.3\text{cm}$ $L_{c-w}=11.5\text{cm}$ $L_{w-p}=2.8\text{cm}$ $L_{p-p}=2.2\text{cm}$	$C=8.4\text{cm}$	Length : $L_{g-e}=8.38\text{cm}$ $L_{e-c}=10.18\text{cm}$ $L_{c-w}=11.3\text{cm}$ $L_{w-p}=2.7\text{cm}$ $L_{p-p}=2.26\text{cm}$
2	Male, 5 years old, vaccinated	4.3kg	$L_{g-e}=8.5\text{cm}$ $L_{e-c}=10.2\text{cm}$ $L_{c-w}=11.3\text{cm}$ $L_{w-p}=3.0\text{cm}$ $L_{p-p}=2.2\text{cm}$	$C=8.3\text{cm}$	Circumference average : $C=8.16\text{cm}$
3	Female, 6 years old.	4.1kg	$L_{g-e}=8.2\text{cm}$ $L_{e-c}=10.0\text{cm}$ $L_{c-w}=11.2\text{cm}$ $L_{w-p}=2.5\text{cm}$ $L_{p-p}=2.3\text{cm}$	$C=8.1\text{cm}$	
4	Female, 4 years old.	3.8kg	$L_{g-e}=8.2\text{cm}$ $L_{e-c}=10.0\text{cm}$ $D_{c-w}=11.2\text{cm}$ $L_{c-w}=2.6\text{cm}$ $L_{w-p}=2.4\text{cm}$	$C=8.0\text{cm}$	
5	Female, 4 years old.	4.5kg	$L_{g-e}=8.5\text{cm}$ $L_{e-c}=10.5\text{cm}$ $L_{c-w}=11.3\text{cm}$ $L_{w-p}=2.6\text{cm}$ $L_{p-p}=2.2\text{cm}$	$C=8.0\text{cm}$	

III. RESULTS

The EMG sensor used is a prototyping model which is not sophisticated for biomedical equipment. It is characterized by the presence of

an operational amplifier, which filters and amplifies the signal. It contains three inputs to connect it to the battery and two outputs to connect it to the Arduino uno board. Muscular activity was measured following the steps described above for a cat: In the figure 4, the ECG artefact and other artefacts related to the movements of the electrodes appear repeatedly.

The amplitude of the muscle signal during concentric contraction of the *biceps brachii* varied from 640 to 700 au, i.e. an absolute amplitude of 10 au. The baseline characterizing the resting potential takes on a stable value of 660 au. Any small fluctuation around the baseline are not interpreted as an EMG signal.

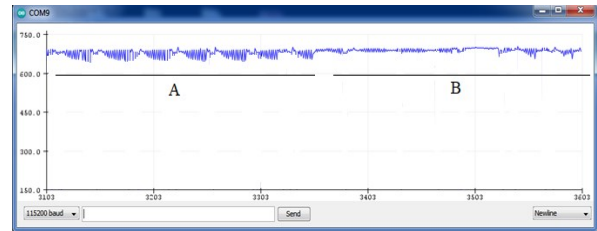


Fig. 4. Graph obtained by the EMG V3 sensor arduino module for a delay of 50. (A): action potential during noisy concentric contractions. (B): resting potential in the absence of contraction when the arm is relaxed.

Figure 5 is photography of the assembled prototype.

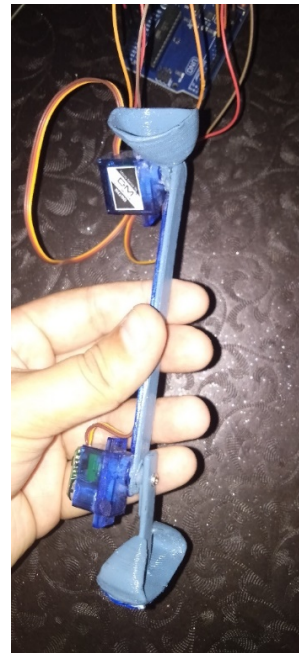


Fig. 5. Close-up of the assembled exoprosthesis.

IV. CONCLUSION

We have successfully developed a bionic prototype for the left forearm in cats. Nevertheless, when obtaining measurements of the limb's dimensions, we discovered that relying solely on data from healthy cats does not adequately represent the dimensions of a cat with a forelimb amputation. To create a high-performance model, it is imperative to consider the stump's conformation by utilizing a model. It should be noted that the myoelectric signal measurements from the biceps during a concentric contraction in a normal cat could not be used for programming the bionic limb. This is due to the stark contrast in muscle condition between a healthy cat and one with an amputated forearm.

Regrettably, the assessment of the prototype's performance on an amputee cat was not possible due to COVID-related restrictions, which limited the duration of clinics at the school. Consequently, we missed the opportunity to evaluate the prosthetic's efficacy on a feline with a forelimb amputation. In addition to the aforementioned challenges, we identified issues with the design and material (GPET) used in the insert. The current design appears excessively rigid to be comfortably fitted onto a stump, posing a significant risk of skin injury due to frequent pressure and shearing. A potential solution in this case would involve a more pliable liner composed of inert materials like polyurethane or silicone, or their derivatives (Cagle et al., 2018).

Concerning the servomotors we employed, it is worth noting that their configuration is better suited for robotics rather than biomedical prototyping, as indicated by the manufacturer (Gràcia, 2015). The motor's power is not the only parameter to be taken into consideration, but also its weight.

In fact, a prosthesis that is too heavy would be difficult for a small carnivore like the cat to wear, and increasing the asymmetrical weight of one region of the body would shift the center of mass (COM), which will influence the animal's postural and dynamic balance to secure the prosthesis onto the animal's stump. We have explored two

options: the use of a support belt, akin to certain limb prostheses in the canine species (Mich, 2014), or adjustable attachment straps that rest on the animal's shoulders. Alternatively, a promising solution might be achieved by integrating the prosthesis with a trans-humeral implant (Jarrel & Farrel, 2018). While the current bionic limb prototype does not exhibit significant weight, it is essential to consider the additional electronic components, including the microcontroller, batteries, and EMG sensor, which could potentially increase its overall mass.

To mitigate this, wireless connectivity options can be explored. In human bionic engineering, solutions like sEMG and near-infrared (NIR) coupling bracelets have been employed successfully. These transmit the myoelectric signal (detected by EMG electrodes) and position-related data (sensed by infrared sensors) of the limb via Bluetooth to the microcontroller, effectively reducing the bulk associated with traditional electrode and cable setups (Nsugbe et al., 2020).

It is worth noting that there are more compact and lightweight microcontroller models, such as the Arduino Nano, which could be considered for future prototypes.

V. REFERENCES

- [1] Cabibihan, J. J., Abubasha, M. K., & Thakor, N. (2018). A method for 3-d printing patient-specific prosthetic arms with high accuracy shape and size. *IEEE Access*, 6, 25029-25039.
- [2] Cagle, J. C., Hafner, B. J., Taffin, N., & Sanders, J. E. (2018). Characterization of prosthetic liner products for people with transtibial amputation. *JPO: Journal of Prosthetics and Orthotics*, 30(4), 187-199.
- [3] Capell Gràcia, A. (2015). Design and implementation of a bionic arm (Bachelor's thesis).
- [4] Durfee, W. K., & Iaizzo, P. A. (2019). Medical applications of 3D printing. In *Engineering in medicine* (pp. 527-543). Academic Press.
- [5] Ishmael, M. K., Tran, M., & Lenzi, T. (2019, June). ExoProsthetics: Assisting above-knee amputees with a lightweight powered hip exoskeleton. In *2019 IEEE 16th International Conference on Rehabilitation Robotics (ICORR)* (pp. 925-930). IEEE.
- [6] Jarrell, J. R., Farrell, B. J., Kistenberg, R. S., Dalton, J. F., Pitkin, M., & Prilutsky, B. I. Kinetics of individual limbs during level and slope walking with a unilateral

- transtibial bone-anchored prosthesis in the cat. *Journal of Biomechanics*, 2018, (76), 74–83.
- [7] Konrad, P. (2005). *The abc of emg. A practical introduction to kinesiological electromyography*, 1(2005), 30-5.
- [8] Mich, P. M. (2014). *The emerging role of veterinary orthotics and prosthetics (V-OP) in small animal rehabilitation and pain management. Topics in companion animal medicine*, 29(1), 10-19.
- [9] Nayak, C., Singh, A., & Chaudhary, H. (2017). *Customized Design and Development of Transtibial Prosthetic Socket for Improved Comfort Using Reverse Engineering & Additive Manufacturing (Doctoral dissertation, Ph. D. Thesis, MNIT, Jaipur)*.
- [10] Nsugbe, E., Phillips, C., Fraser, M., & McIntosh, J. (2020). *Gesture recognition for transhumeral prosthesis control using EMG and NIR. IET Cyber-Systems and Robotics*, 2(3), 122-131.
- [11] Wu, X., Pei, B., Pei, Y., Wu, N., Zhou, K., Hao, Y., & Wang, W. (2019). *Contributions of limb joints to energy absorption during landing in cats. Applied Bionics and Biomechanics*, 2019.